Summer 2017

The Effect of Bone and Ligament Morphology of Ankle Joint Loading in the Neutral Position

Jinhyuk Kim
Old Dominion University, jkimx024@odu.edu

Recommended Citation

THE EFFECT OF BONE AND LIGAMENT MORPHOLOGY OF ANKLE

JOINT LOADING IN THE NEUTRAL POSITION

by

Jinhyuk Kim
B.S.M.E. May 2014, Old Dominion University

A Thesis Submitted to the Faculty of
Old Dominion University in Partial Fulfillment of the
Requirements for the Degree of

MASTER OF SCIENCE

MECHANICAL ENGINEERING

OLD DOMINION UNIVERSITY
August 2017

Approved by:

Stacie I. Ringleb (Co-Director)

Sebastian Y. Bawab (Co-Director)

Gene Hou (Member)

ABSTRACT

THE EFFECT OF BONE AND LIGAMENT MORPHOLOGY OF ANKLE JOINT LOADING IN THE NEUTRAL POSITION

Jinhyuk Kim
Old Dominion University, 2017
Co-Directors: Dr. Stacie Ringleb
Dr. Sebastian Bawab

Computational modeling of joints is used to investigate the effect of injuries, to plan surgeries, and to answer questions about joints that cannot be answered experimentally. Existing models of the ankle joint are moving toward being able to model specific patients, however, they do not include all of the anatomy (e.g., bones and/or ligaments) and have restrictive boundary conditions. These simplification in anatomy are made to minimize pre-processing and computation time. Because biomechanical modeling is increasingly focused on the implementation of patient specific cases, the effects of including more anatomical structures and determining how they affect the model results is necessary. Therefore, the purpose of this study was to develop a 3D Finite Element (FE) model of the ankle joint complex (i.e., tibia, fibula, talus, and calcaneus) with 13 major ligaments, and to determine how modeling the structure of the ligaments and the number of bone affected the contact stress in the talocrural joint (i.e., the joint between the tibia/fibula and the talus). A finite element model was developed in FEBio (FEBio, Salt Lake City, UT) from the CT data obtained from one cadaver. The model included bones, cartilage, and ligaments. Ligaments were modeled as tension-only linear springs, and applied for more than one spring for each of 13 major ligaments. Morphology of the spring was set as parallel or X configuration. The stress in the joint between the tibia and talus showed differences with the different number of bones. Especially, the stress of the three bone FE model was higher than ankle complex configuration with the same number of ligaments. The stresses were measured in Talocrural Joint 2 including tibia, talus, and 6 springs and Talocrural Joint 3 including tibia, talus, fibula, calcaneus, and 12 springs from 2.0541 MPa to 2.3077 MPa. The big difference between the models was the existence/non-existence of calcaneus. It demonstrates that the stress contour of Talocrural Joint 3 was had the most similar pattern with the Novel pressure data obtained from experiment.

This thesis is dedicated to my family: Minju, Justina, Olivia
Mr. Duk Song Kim, and Mrs. Jae Soon Jung.

ACKNOWLEDGMENTS

TABLE OF CONTENTS

LIST OF TABLES

LIST OF FIGURES

Page

CHAPTER I

INTRODUCTION

Computational modeling of joints is used to investigate topics including, but not limited to the effect of injury, plan surgeries, and to improve our understanding of the functional behavior of ankle joints and ankle ligaments [1, 2]. It is also useful to the figure out tissue and body scales and to investigate the ability of body and tissues to stabilize the joints during gait. In addition, this can help reduce the experimentation time because the joints are tested under a variety of circumstances [3]. 3D Finite Element (FE) models are useful in biomechanics to investigate multi-body dynamics or static analysis of stress and pressure in joint joints [4, 5]. Furthermore, the FE modeling is convenient for surgical planning and prediction of clinical or surgical evaluation because it is provided for the appearance the deformation of the joint [6, 7].

1.1 Previously Published Finite Element Models

In the past, finite element models of the ankle were created to examine the stress, strain, and pressure between the tibia and talus. The FE models were also used to evaluate the effects of ligaments, tissues, and bones because it was hard to define and measure the capabilities and functions in a real foot. Thus, the FE model composed of bones, cartilages, muscle force, or ligaments was assembled to simulate the gait of human, the accidental motion of the foot, and the effect of artificial joint. Results of the simple 3D FE models were in agreement with the experimentally measured data. Unfortunately, the complicated 3D FE models did not consistently agree with the experimentally measured results. The detailed information is explained below.

1.2 Validation of Subject Specific Model

A FE model including the distal segment tibia, talus, cartilages, and one ligament was constructed [8]. A single linear spring, which was modeled to represent a non-anatomic ligament in the 3D model, was used to resist anterior-posterior translation of an ankle joint. Plantarflexion and dorsiflexion were fixed, but inversion and eversion were free to rotate. The distal segment tibia was not constrained in translational motion (Figure 1). The articular cartilage was created along local bone surface, having a uniform thickness of 1.7 mm. TrueGrid software (XYZ Scientific Applications Inc., Livermore, CA) was used to generate all-hexahedral FE mesh for the bone and cartilage. The FE ankle contact stresses were analyzed using ABAQUS 6.6. Then, the experimental ankle contact stresses were measured with a Tekscan pressure sensor (Tekscan, Inc., South Boston, MA). The frozen cadaver ankles were tested in the neutral load-bearing joint apposition fixed by the stainless steel K-wires drilled across the joint [8].
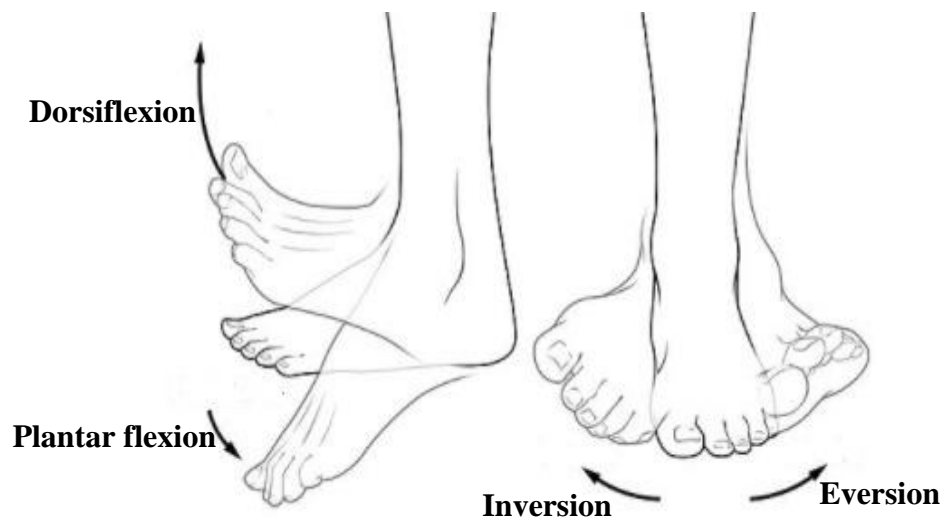
Figure 1 The images for foot and ankle joint's movements of a left foot. Dorsiflexion is that foot moves towards chest. Plantar flexion is that foot moves downward. Inversion moves the foot inward from the midline. Eversion moves the foot outward from the midline [9].

The experimental and FE model contact stress results showed stress acting on the lateral half of the tibial surface. In the experimental circumstance, the maximum contact stress for experimental was 3.69 MPa on 295.1 mm^2 contact area. The maximum contact stress in the FE model was measured 3.74 MPa on the 290.5 mm^2 contact area [8]. The experimental contact stress result was coincided with the numerical contact stress under the limited circumstances. The use of K-wires fixing the tibia to the talus dedicated to avoiding complicated ankle motion, far from a real ankle analysis problems. Furthermore, a ligament was replaced with only one linear spring serving as anterior/posterior tibiotalar ligaments. Even though the FE model wasn't anatomically correct, the stress distributions were still similar to the physical experiment's results.

1.3 Validation of Ankle Arthroplasty

A FE model including the distal segment tibia, fibula, talus, calcaneus, interosseous membrane, and eight major ligaments, anterior talofibular, posterior talofibular, tibionavicular (TiNa), deep anterior tibiotalar, deep posterior tibiotalar, superior tibiotalar, calcaneofibular (CaFi), tibiocalcaneal (TiCa) ligaments, was modeled to validate the two different artificial joints [10].The FE model was created to investigate the contact stress and to develop Agility^{TM} and S.T.A.R.^{TM} total ankle replacements. The main purpose was how to remodel bone for ankle joint. The ParaView (Sandia Corporation, Kitware Inc., NM, USA), ABAQUS, and Solidworks (Dassault Systemes SOLIDWORKS Corp., Waltham, Mass) software were used to create the smooth surface and to analyze the contact stress. The bones were assigned linearly elastic, heterogeneous, and isotropic linear elastic material properties (E = 19000 MPa or 500 MPa, v = 0.3). Cartilage was modeled as an isotropic linear elastic material properties (E = 1 MPa, v = 0.4). The boundary condition and stiffness of spring were not mentioned. The eight ligaments with

unmentioned properties by author were modeled as a tension-only truss element. The connection between tibia and fibula was connected rigidly by interosseous membrane. Also, the FEM was considered in three different positions such as dorsiflexion, neutral, and plantarflextion position. Then, three different load cases, 400N, 600N, and 1600N were applied to the three different positions, 15° plantarflextion, neutral, and 10° dorsiflexion positions. In this case study, it was shown that the contact stress could be changed by the different positions. According to the three different positions with three loading cases, it helps to understand the changing stress contour during gait.

The results were compared with the result of Anderson et al. when 600N axial force were applied [8]. The maximum contact stress was 3.95 MPa at neutral position. The results were similar to the model described in Section 1.1. The FE model which includes bones and eight major ligaments was not validated, but the maximum contact stress and mean contact tress were similar to that predicted and measured by Anderson et al.

1.4 Validation of Anatomical Finite Element Ankle Model

A FE model including ankle bones, cartilages, ligaments, and tendons was modeled to investigate the contact stress as anatomical ankle motion during gait [11]. For collecting the experimental data, a custom horizontal loading device was used in order to measure articular joint pressure and collect kinematic data obtained from one cadaver ankle with unknown age and sex, which was a left foot. A Pliance Ankle Sensor (Novel Electronics Inc.) was used to collect and analyze the contact tress in the joint. Commuted Tomography (CT) images were used to develop a FE model. The CT images were exported as Digital Imaging and Communications in Medicine (DICOM) files, and imported into AVIZO 6.3 (Visualization Sciences Group, Burlington, MA). Rhinoceros 3D (Robert McNeel & Associates, Seattle, WA), Geomagic

(Geomagic Inc. Morrisville, NC) were used to created points and smooth surface for each of the bone, then the files were saved as the Initial Graphics Exchange Specification (IGES) files. The files were then imported into LS-DYNA (LSTC, Livermore, CA) to produce a FEM. The cartilages of 1.06 mm thickness were uniformly created along local bone surface. The 1.06 mm thickness of cartilage was chosen because of the sum of the half of the space between the bones. The tibia and fibula were rigidly connected by a spring. The sliding interface was applied to the tibia and talus. Then, other bones were connected rigidly by tied interface. Also, the six major ligaments without any citation, anterior tibiotalar (ATT), posterior tibiotalar (PTT), tibioncalcaneal (TiC), anterior talofibular (ATaF), posterior talofibular (PTaF), calcaneofiblar (CF), and were applied to constrain the tibia and talus. The model was solved in three different positions, 10°dorsiflexion, neutral, and 10°, and 20° plantar-flexion position.

The 40 lbs axial force was applied to tibia and tendon. A load was applied to the major tendon including anterior tibialis (AT), posterior tibialis (PT), extensor halluces longus (EHL), extensor digitorum longus (EDL), peroneus brevis (PB), peroneus longus (PL), flexor halluces longus (FHL), flexor digitorum longus (FDL), and the achilles tendon as an axial load for all three position cases [11]. The experimental peak pressure ranges were from 1.94 to 2.55 MPa. The peak pressure of FEM ranges were 1.7 to 2.8 MPa in three different positions. The peak pressure of the Pliance novel sensor at neutral position was 1.94 MPa at the anterior, but the peak pressure of FEM was 2.8 MPa. The peak pressures at 10° plantar-flexion position as 2.55 MPa, and 1.7 MPa for FEM model and experimental data. The peak pressures at 10° dorsiflexion position was 2.5 MPa and 1.97 MPa for FEM model and experimental data. In this study, the ligaments were modeled as single spring elements. The stiffness of spring for interosseous talocalcaneal ligaments was not in the literature, so the unknown stiffness of spring was assumed

100N/mm. Also, the applied boundary conditions and contact method on articular joint to 3D FE models were not clearly defined in the paper. Furthermore, the results of stress contour pattern were not similar to the experimentally measured data.

1.5 Objective
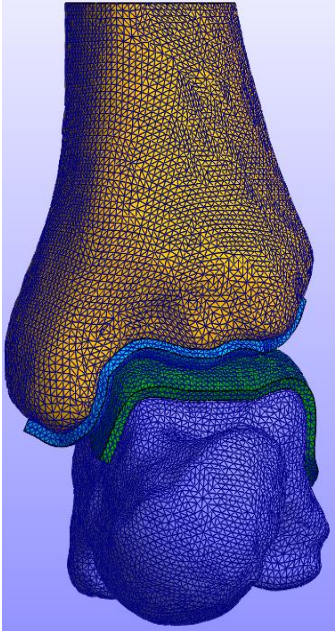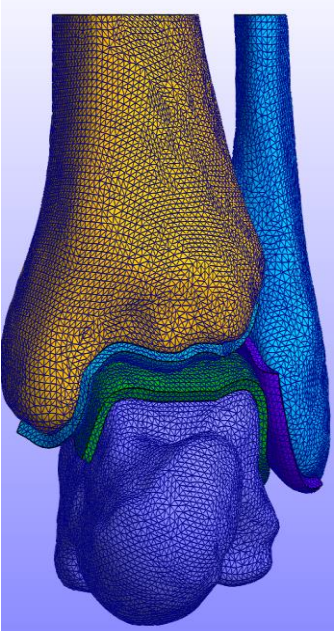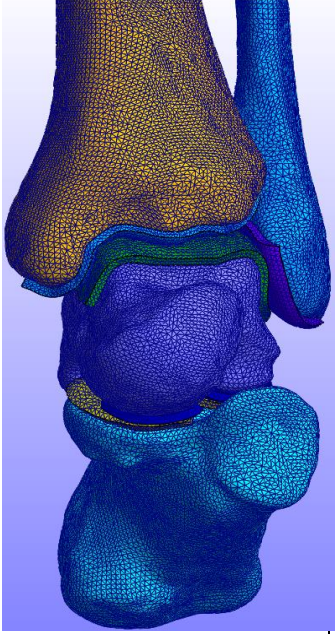
The aforementioned studies had various approached to the complexity of modeling the ankle, with the shared goal of producing valid, patient specific models. Specifically, the model developed by Anderson et al. [8] only contained two bones and one ligament, while the model developed by Dong included all bones in the foot and ankle (with contact modeled in a few joints), all major ankle ligaments, as well as forced to simulated tendon loads [11]. With the trend toward using subject-specific models, it is critical to understand how much detail patient specific models should include. Therefore, the main purpose of this study is to determine how the number of bones and ligaments as well as the morphology of ligaments models affects the contact stresses in the talocrual joint. This was completed by creating three major models of the ankle joint: 1) tibia and talus, 2) tibia, fibula, and talus, and 3) tibia, fibula, talus, and calcaneus in FEBio (University of Utah, Salt Lake City, UT). Each model examined various boundary conditions and ligaments morphologies (e.g., how many springs should be used to model a ligament).

CHAPTER II

METHODS

In this study, the FE models simulated the effect of ligaments and the number of bone in the neutral position of the ankle. FEBio was used to develop a finite element model including tibia, fibula, talus, calcaneus, cartilages, and ligaments. For each model 1) it was assumed that a ligament was linear elastic springs; 2) the thickness of cartilage is 1.7 mm uniformly constant; 3) a 600N axial nodal load was applied; 4) the load linearly increases over a second; 5) the density of bone (E = 13,000 MPa and $v = 0.3$) and cartilage (12 MPa and $v = 0.42$) are constant; 6) the cartilage was rigidly fixed to the bone; 7) the stiffness of ligaments ranged from 10 to 100 N/mm; if the value is unknown (40 N/mm stiffness was applied). The following models were created; 1) tibia and talus with a sliding interface (Talocrural Joint 1); 2) tibia, talus, and fibula with a sliding interface (Talocrural Joint 2); 3) tibia, talus, fibula, and calcaneus with a sliding interface (Table 1).

Table 1 Three types of bone configurations in the neutral position. The tibia is shown in yellow, the talus is shown in purple, the fibular is shown blue, and the calcaneus is shown in bright blue.

	Talocrural Joint 1	Talocrural Joint 2	Ankle Joint Complex
FE Model	Tibia Talus	Tibia Fibula Talus	Tibia Fibula Hindfoot
Construction			
Number of Nodes and Elements	Nodes: 21774 Elements: 70612	Nodes: 26968 Elements: 86885	Nodes: 43371 Elements: 140878

2.1 Creating Cartilage

Articular cartilage was added to the FE model. The average anatomical cartilage thickness ranged from 2.38±0.4mm or 1 to 1.7mm [2, 12]. Thus, the articular cartilage was assumed to be a uniformly thin layer. The 1.7 mm thickness was also chosen for the cartilage after comparing with other results [5, 6]. The cartilages were created as solid face elements in LS-Prepost 4.0 with triangular and quadrilateral meshes, and extended between bone shells based on the CT scans with a uniform thickness of 1.7 mm (Figure 2). The created cartilages were tied to their respective surface on bone.

| (a) Tibia | (b) Tibia-Cartilage | (c) Tibia-Cartilage |
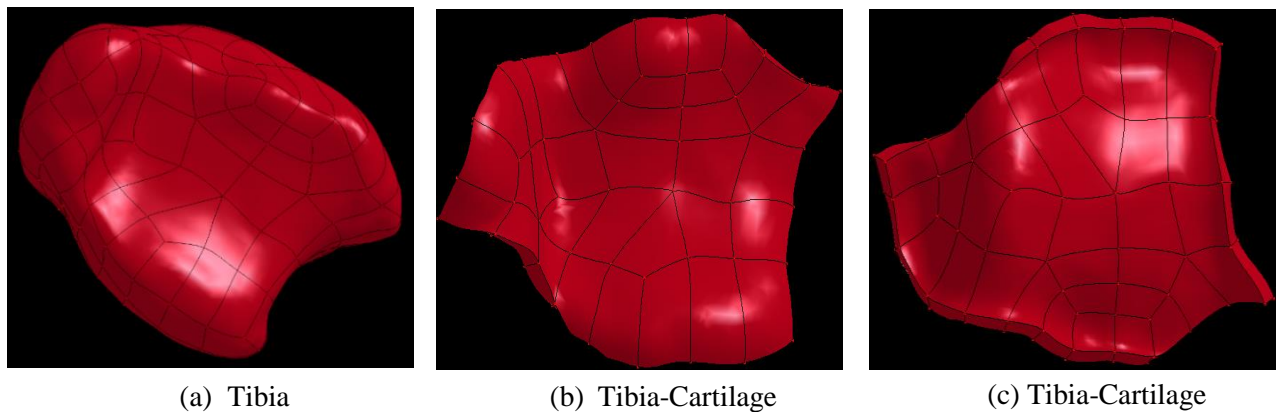
Figure 2 Example for creating cartilage from a tibia. These are the inferior and superior views of the tibia and cartilage.

2.2 Meshing

In Visual Mesh DYNA 7.5, meshes were created by the aid of the specific function of the software named 2D Auto-mesh Surfaces, which uses quadrilateral mesh [13]. Automatic mesh generation helped to improve mesh quality [14]. The surface of bone segments were discretized into quadrilateral shell elements. The number of nodes was automatically decided to create smooth and high quality mesh surface using the function of automatic surface mesh (Figure 3). Cartilages were also imported into Visual Mesh DYNA 7.5 to discretize into quadrilateral solid elements (Figure 3). Each node number of a cartilage was manually matched to that of a bone to contact the surfaces (Figure 4). Using the auto-mesher, the number of elements for bone was ranged from 12617 to 40584. For the cartilage, the number of elements was ranged from 3646 to 17270 (Table 2).

(a) CT-Based geometry Surface   (b) Finite element mesh
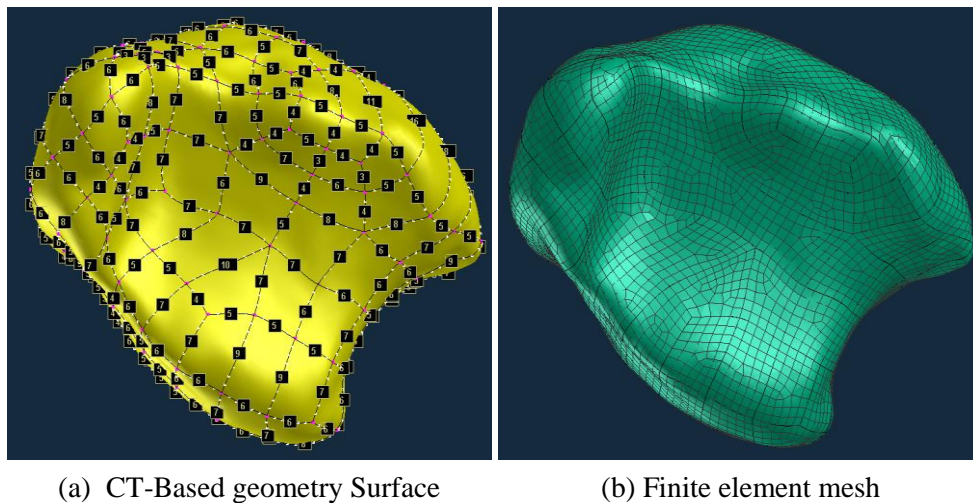
Figure 3 (a) Geometry surface of tibia and (b) finite element mesh of a tibia using automatic mesh generation.

(a) CT-based geometry surface   (b) Finite element mesh of cartilage
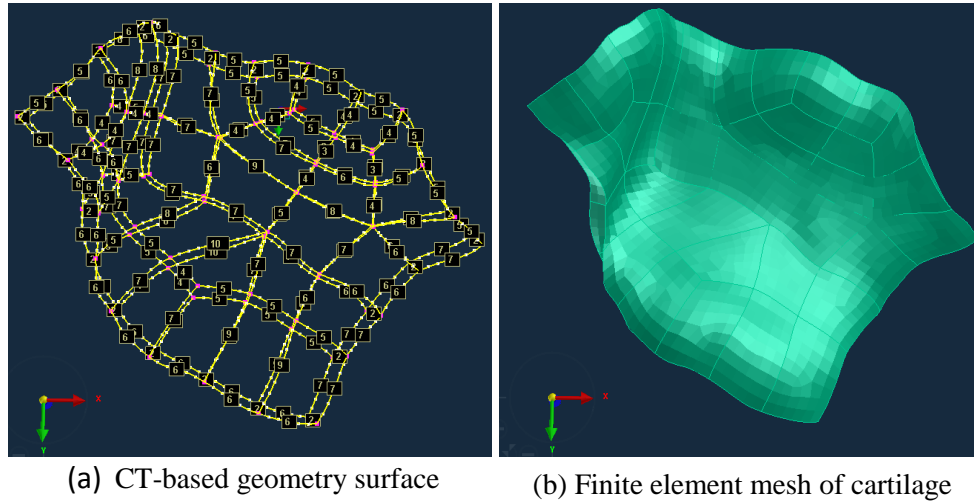
Figure 4 (a) Geometry surface of tibia's cartilage and (b) finite element mesh of tibia cartilage created using automatic mesh generation.

Table 2 Number of elements for each bone and cartilage

	Number of Elements
Tibia	26,986
Talus	26,575
Calcaneus	40,584
Fibula	12,617
Cartilage, Fibula	3,646
Cartilage, Tibia	7,833
Cartilage, Talus	17,270
Cartilage, Calcaneus	8,923

2.3 Material Properties

The bones included tibia, talus, fibula, and calcaneus were modeled as isotropic elastic model. The isotropic elastic material is widely used to represent human bones because the deformation of bone can be negligible [11, 15]. In FEBio, a rigid body is more sensitive to the rotation than isotropic elastic material, therefore additional extra boundary conditions were required for a model to converge when the bones were modeled as rigid bodies, even though the same FE models were utilized [16]. For this reason, isotropic elastic material models were used to make and compare the finite element model for the ankle [17].

For the cartilages, FEBio Software Suite provides a number of nonlinear constitutive models. Neo-Hookean, Mooney-Rivlin, and isotropic elastic can be used for complicated biological cartilage [18]. Neo-Hookean, isotropic elastic, and Mooney-Rivlin showed similar stress patterns. However, the Mooney-Rivlin model produced the largest error in the compression load test [19]. Therefore, the Neo-Hookean hyperplastic model was used so that the cartilage can be created as finite element model. The properties of bone and cartilage are shown in Table 3.

Table 3 Material properties for bone and cartilage. Isotropic elastic was applied to bone segments.

Part name	FEBio	Density (kg/mm^3)	Young's Modulus (GPa)	Poisson's Ratio	Reference
Bone	Isotropic Elastic	4.65E-6	13	0.3	[11]
Cartilage	Neo-Hookean	1.93E-6	0.012	0.42	[8]

2.4 Finite Element Model

The original Computed Tomography (CT) images of the tibia, fibula, talus, and calcaneus were obtained and segmented in a prior study [11]. The CT data were turned into the surface using AVIZO 6.3 (Visualization Sciences Group, Burlington, MA). In the present study, Visual-Mesh DYNA 7.5 (ESI Group Company North America, Columbia, MD) was used to create new Stereo Lithography (STL) files for each bone. The smooth mesh surface created by Visual Mesh DYNA 7.5 was imported into FEBio (Figure 5). The imported triangular and quadrilateral mesh surface of bones and cartilage was automatically set as a 3-node linear triangles (TRI3) in FEBio. Initial simulations failed due to a Jacobian Error, therefore, the TRI3 mesh type was replaced with 4-node quadratic tetrahedral element (TET4) by the function of Tetrahedral Mesh Generation (TetGen) in FEBio (Figure 5).
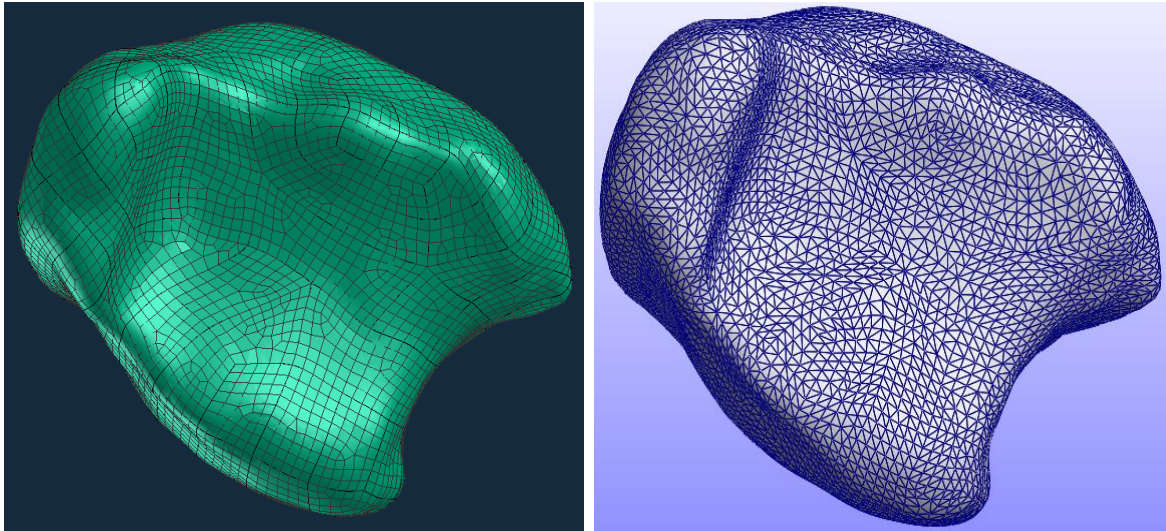
(a) Meshing in Visual Mesh DYNA   (b) Meshing in FEBio

Figure 5 Inferior views of the tibia, after (a) meshing in Visual Mesh DYNA (before TetGen) and (b) being imported into FEBio (after TetGen)
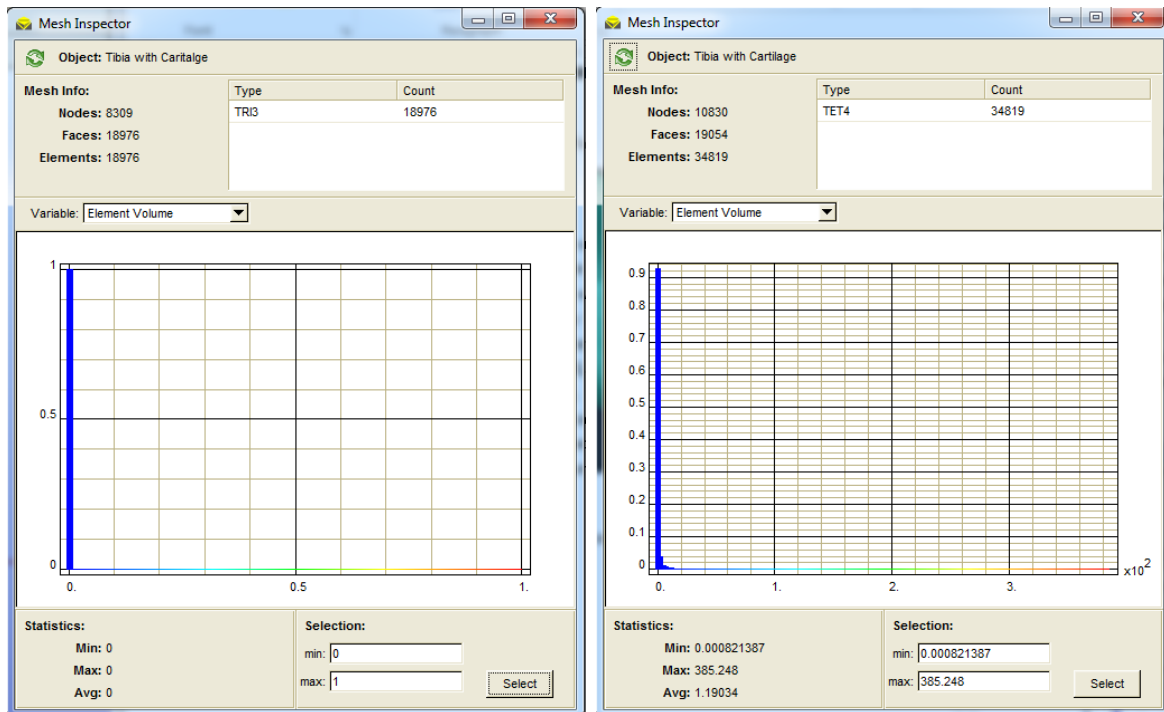
(a) Meshed Element in Visual Mesh DYNA   (b) Meshed Element in FEBio

Figure 6 The mesh type represented TRI3 when the quadrilateral mesh was imported into FEBio (a), the TRI3 mesh type was converted into TET4 using Tetrahedral mesh Generation (TetGen) in the FEBio (b), therefore, the number of nodes, faces, and elements were increased.

2.5 Boundary Conditions and Load

The 3D finite element model was modeled as an isotropic elastic body. The boundary conditions were defined based on how contact was modeled, material type, number of ligaments, and number of bones. The application of boundary condition is shown in Figure 7. The boundary conditions for each bone segment were changed depend on the number of bone (Table 4). In this study, the moments were neglected between cartilage surfaces. Thus, load was defined as an axial nodal force and 600N applied at a reference point located in the edge of the tibia and fibula. The axial nodal force was constantly increased during one second.

600 N axial nodal force

Fixed Nodes in 6 DoF
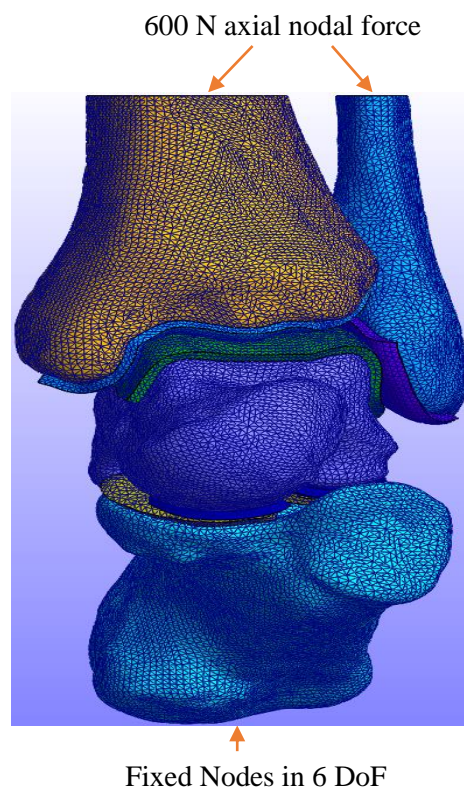
Figure 7 The finite element model of ankle joint complex and application of boundary conditions. The calcaneus was fixed in six degree of freedom (DoF). The 600N axial nodal force was applied on the edge of tibia and fibula and the load was smoothly increased from 0N to 600N during one second.

Table 4 The list of the boundary conditions is what boundary conditions were applied to the each bone. There are three bone configurations for defining boundary conditions with the number of ligaments.

FE model	Bones	Boundary Conditions	Total Number of Ligaments
Talocrural Joint 1	Tibia	Fixed X-direction, Fixed Y-direction, Fixed XY-direction, Fixed XY and Rx, Fixed XY and RxRy, or Fixed XY and RxRyRz	2 tension only linear springs
	Talus	Fixed 6 DoF	
Talocrural Joint 2	Tibia	Fixed X-direction	6 tension only linear springs
	Talus	Fixed 6 DoF	
	Fibula	Fixed X-direction	
Ankle Joint Complex	Tibia	Fixed X-direction	13 tension only linear springs
	Talus	None	
	Fibula	Fixed X-direction	
	Calcaneus	Fixed 6 DoF	

2.6 Cartilage Attachment and Contact Interaction

A surface between bone and cartilage was not perfectly matched therefore the slave surface was adjusted in order to prevent itself from penetrating the master surface. Thus, the tolerance between bone and cartilage was ranged from 0.1mm to 0.3mm. Generally, the tied contact interface is useful for connecting two non-conforming meshes together. However, this method does not model anatomic ankle motion. Therefore, the sliding contact-interface was applied between two cartilage layers to obtain more realistic human ankle motions.

The sliding contact interface between two cartilage layers was defined using a facet-to-facet sliding contact interaction. The facet-to-facet sliding interface was useful because the sliding interface was used to remove penetration of surface between two cartilage's surfaces to the sliding with gaps implementation. Thus, the facet-to-facet sliding interface was modeled between tibia and talus and between talus and calcaneus.

2.7 Modeling of a Ligament

In the general anatomy of an ankle, the function of a ligament is stabilizing the ankle joint [19]. Therefore, each ligament has a different shape and its own role. The ankle joint complex models including tibia, talus, fibula, and calcaneus were simulated with the 13 major ligaments which were the: anterior tibiotalar ligament (ATTL), posterior tibiotalar ligament (PTTL), anterior talofibular ligament (ATFL), posterior talofibular ligament (PTFL), tibioncalcaneal ligament (TCL), calcaneofibular ligament (CFL), anterior tibiofibular ligament (ATiFL), posterior tibiofibular ligament (PTiFL), cervical ligament, interosseous talocalcaneal ligament (ITCL), lateral talocalcaneal ligament, posterior talocalcaneal ligament, and medial talocalcaneal ligament. The material properties and cross sectional area for each ligament were from the literature [11, 20-23] (Table 5). Ligaments were represented as tension-only linear springs.

Variations in the models included modeling ligaments with multiple springs proportional to their cross sectional area vs. modeling ligaments as single springs, as well as modeling the ligaments as parallel structures vs. a series of springs modeled like "Xs" in parallel. Table 6 shows the basic spring model for each FE model.
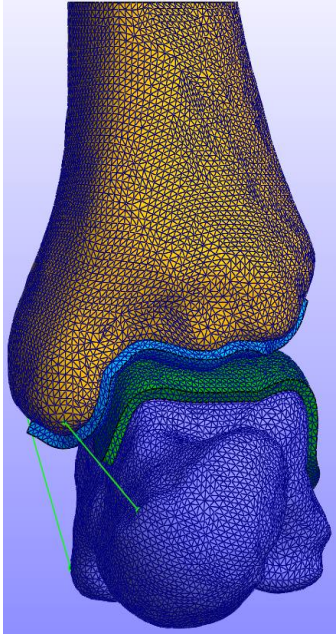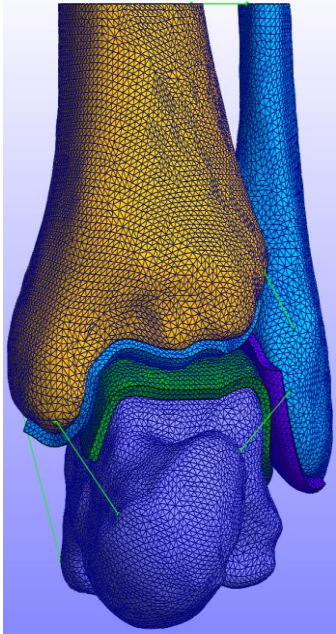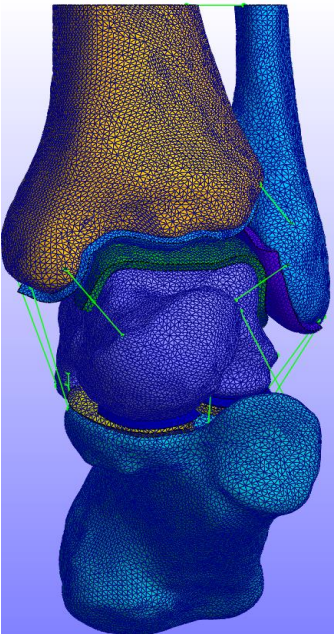
A 20 N/mm stiffness is the minimum stiffness in an ankle ligament and 75.87 N/mm stiffness is highest stiffness in this research. Thus, the stiffness of springs was set to be $10 - 100$ N/mm for talocalcaneal ligaments because there was no reference. In this study, a minimum stiffness of 40 N/mm was necessary to run the analysis successfully. The position of each spring was also placed with anatomical characteristics. The position and width data of ligaments followed other research papers [5, 11, 20].

Table 5 The list of ankle ligament stiffness values and cross section areas included in the model. The number of ligaments was determined depending on the cross section area.

Ligament Name	Spring Constant (KN/mm)	Cross Section Area (mm²)	Number of Ligaments (Spring)	Reference
Anterior Tibiotalar (ATT)	0.025985	43.49±19.92 (6.60±4.46 mm)	2	[20]
Posterior Tibiotalar (PTT)	0.07587	78.43±39.59 (8.86±6.29 mm)	4	[20]
Anterior Talofibular (ATaF)	0.02273	62.85±21.92 (7.93±4.68 mm)	3	[20]
Posterior Talofibular (PTaF)	0.03091	46.43±21.33 (6.81±4.62 mm)	3	[20]
Tibiocalcaneal (TCL)	0.07587	43.20±28.57 (6.57±5.35 mm)	2	[20]
Calcaneofibular (CFL)	0.02063	21.36±7.06 (4.62±2.66 mm)	1	[20]
Anterior Tibiofibular (ATiFL)	0.02273	9.47±2.27 mm	2	[21]
Posterior Tibiofibular (PTiFL)	0.03091	8.94±2.48	4	[21]
Cervical*	0.04	-	4	-
Talocalcaneal Interosseous (ITCL) *	0.04	72.8 (8.53)	4	[5]
Lateral Talocalcaneal*	0.04	6.8 (2.61)	1	[5]
Post Talocalcaneal*	0.04	15.0 (3.87)	1	[5]
Medial Talocalcaneal*	0.04	14.9 (3.86)	1	[5]

*Stiffness of spring was assumed from 10 N/mm to 100 N/mm. Then, a 40 N/mm stiffness was chosen because the stiffness was the minimum stiffness to analyze the FE models with minimum boundary condition.

Table 6 Three types of bone configurations used for model development. Springs are installed in the neutral position

	Talocrural Joint 1	Talocrural Joint 2	Ankle Joint Complex
Bones Included in FE Model	Tibia Talus	Tibia Fibula Talus	Tibia Fibula Hindfoot
3D FE Model			
Number of Springs	2	6	13
Number of Nodes and Elements	Nodes: 21774 Elements: 70612	Nodes: 26968 Elements: 86885	Nodes: 43371 Elements: 140878

2.7.1 Talocrural Joint 1 – Two Bone Model (Tibia and Talus)

The first talocrural joint model consisted of two bones, the tibia and talus, as well as the anterior tibiotalar (ATT) and posterior tibiotalar (PTT) ligaments. The versions of this model varied by increasing the number of springs representing each ligament (i.e., 1 spring = 0 – 22 mm², 2 springs = 22 – 45 mm², 3 springs = 45 – 63 mm², and 4 springs = greater than 63 mm²) and changing the morphology of spring such as parallel or X-configuration (Figure 8).

	Model 1	Model 2	Model 3	Model 4
3D-FE MODEL				
	Model 5	Model 6	-	-
3D-FE MODEL			-	-
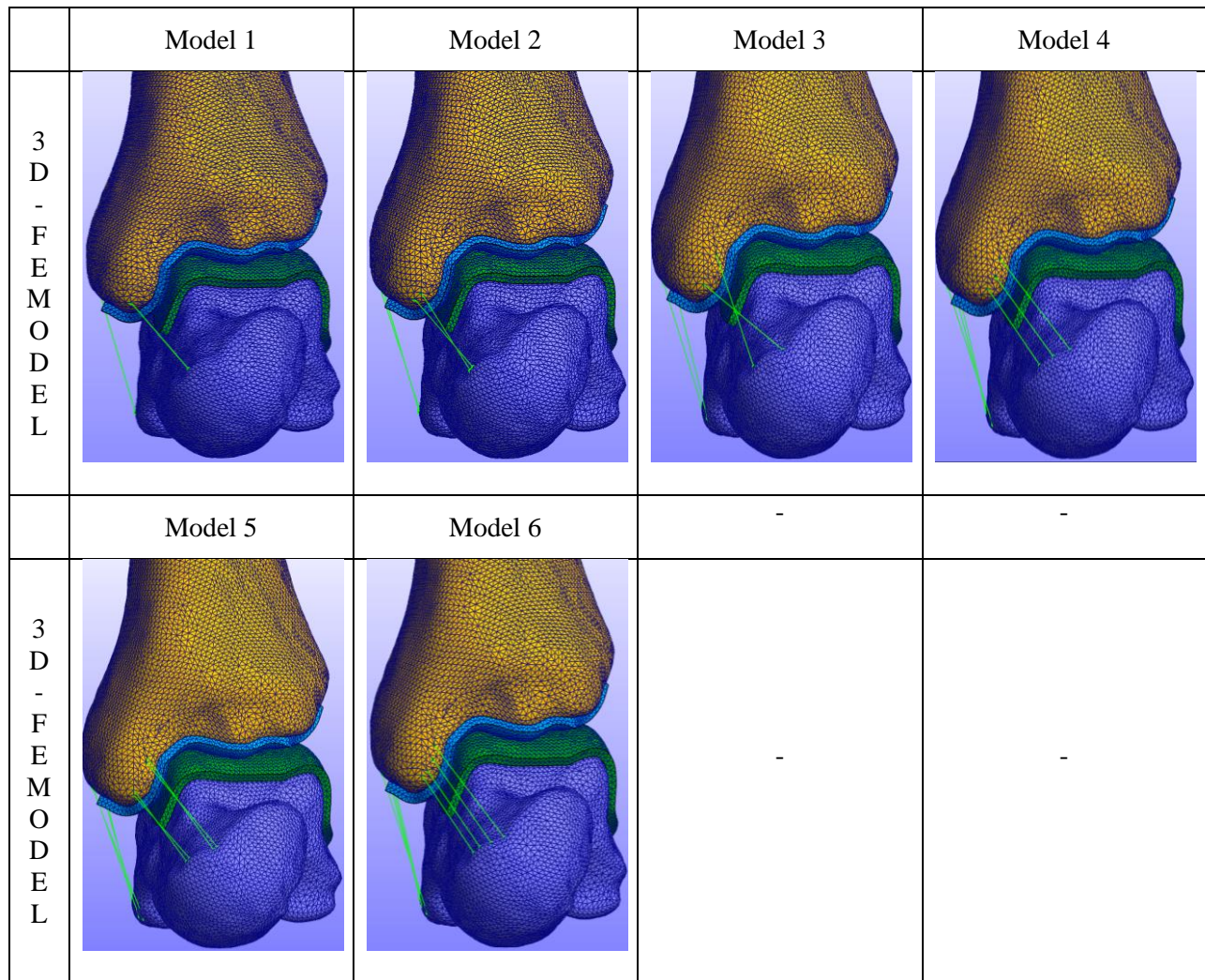
Figure 8 Talocrural Joint 1 was modeled with two springs, anterior tibiotalar (ATT) and posterior tibiotalar (PTT). Two different spring configurations such as parallel and X-configuration were applied to seven distinct ligament's morphologies.

2.7.2 Talocrural Joint 2 – Three Bone Model (Tibia, Talus, and Fibula)

When the fibula was added to the aforementioned model, 6 major ligaments were included: anterior tibiotalar (ATT), posterior tibiotalar (PTT), anterior talofibular (ATaF), posterior talofibular (PTaF), anterior tibiofibular, posterior tibiofibular, were applied for sliding interface method. Ligament morphology was modified by increasing number of springs (i.e., 1 spring = 0 – 22 mm^2, 2 springs = 22 – 45 mm^2, 3 springs = 45 – 63 mm^2, and 4 springs = greater than 63 mm^2), followed by examining the differences between springs modeled in parallel or X-configuration (Figure 9).

	Model 1	Model 2	Model 3	Model 4
3D-FE MODEL				
	Model 5	Model 6	-	-
3D-FE MODEL			-	-
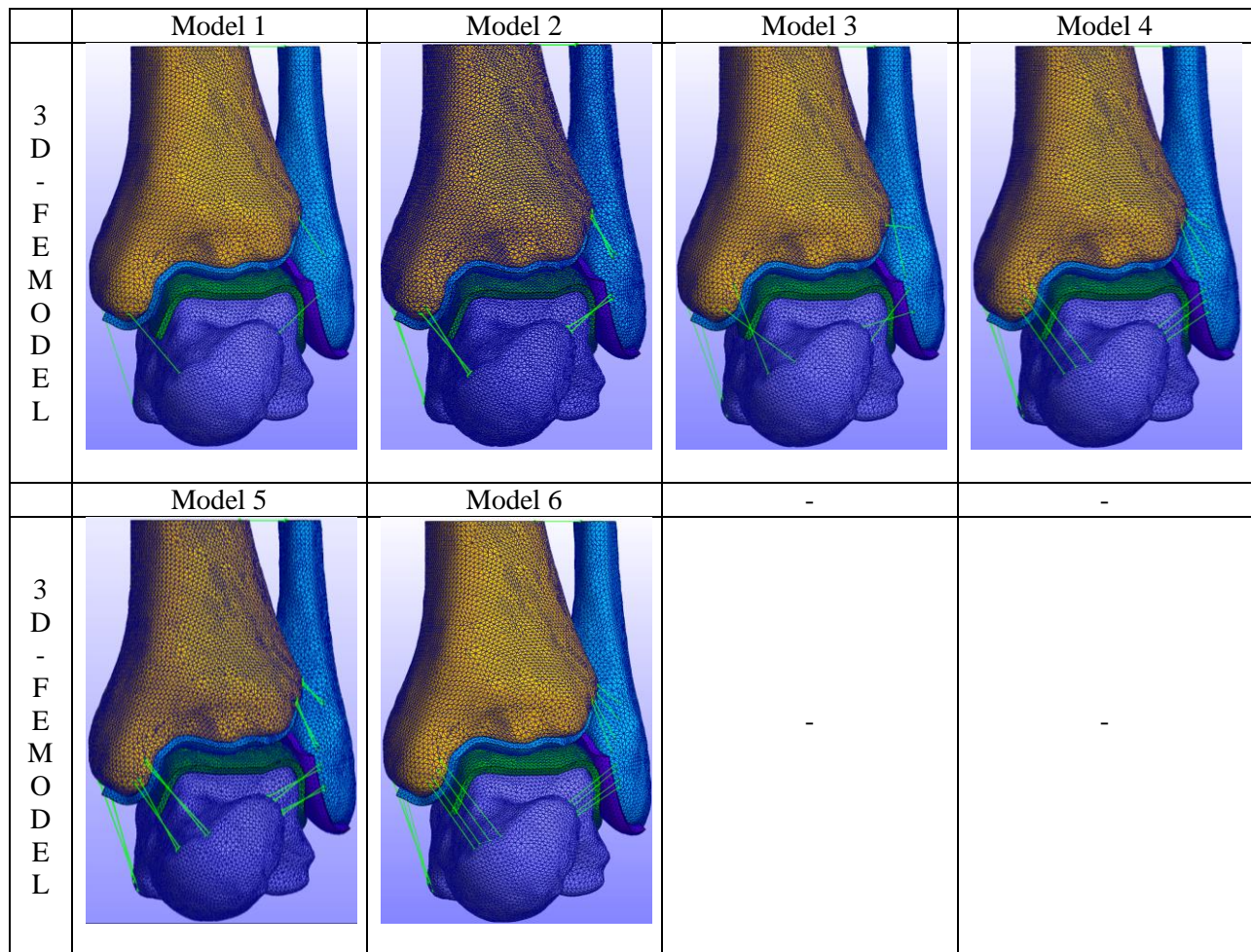
Figure 9 Talocrural Joint 2 modeled with tibia, fibula, talus, and six springs, anterior tibiotalar (ATT), posterior tibiotalar (PTT), anterior talofibular (ATaF), posterior talofibular (PTaF), and anterior tibiofibular, posterior tibiofibular. The springs were set in six different ligament's morphologies such as parallel or X-configuration.

2.7.3 Ankle Complex Joint – Four Bone Model (Tibia, Fibula, Talus, and Calcaneus)

The ankle joint complex model included 13 major ligaments: the anterior tibiotalar (ATT), posterior tibiotalar (PTT), anterior talofibular (ATaF), posterior talofibular (PTaF), tibioncalcaneal (TiC), calcaneofibular (CF), anterior tibiofibular, posterior tibiofibular, cervical, talocalcaneal interosseous, lateral talocalcaneal, post talocalcaneal, and medial talocalcaneal. Similarly to the prior ankle configurations, the number of springs were increased, the number of springs were modeled proportionally to the cross sectional area of the ligaments (i.e., 1 spring = $0 - 22$ mm^2, 2 springs = $22 - 45$ mm^2, 3 springs = $45 - 63$ mm^2, and 4 springs = greater than 63 mm^2), and the results from parallel ligaments were compared to ligaments were compared to ligaments modeled with an X-configuration (Figure 10).
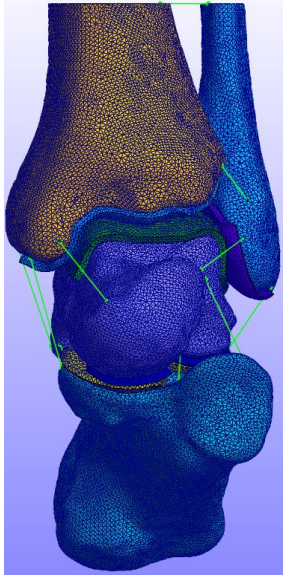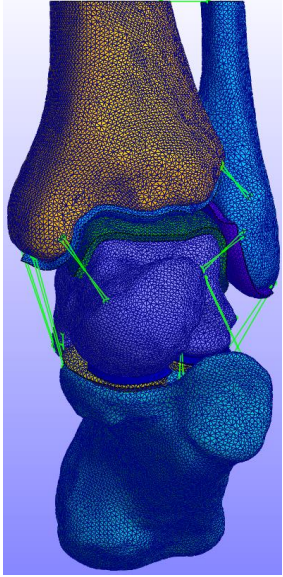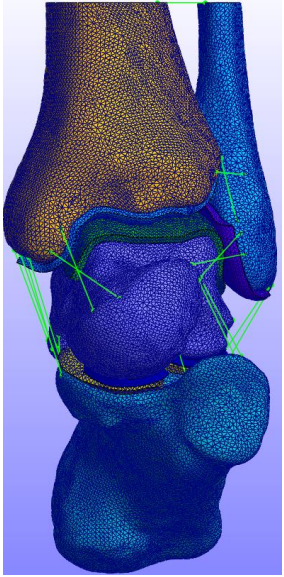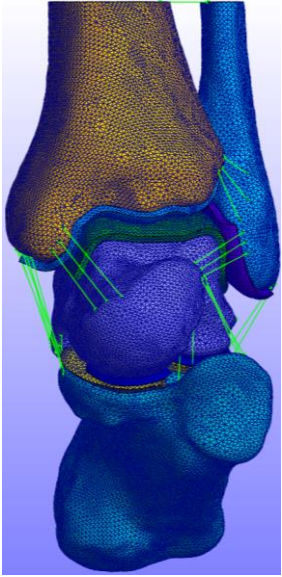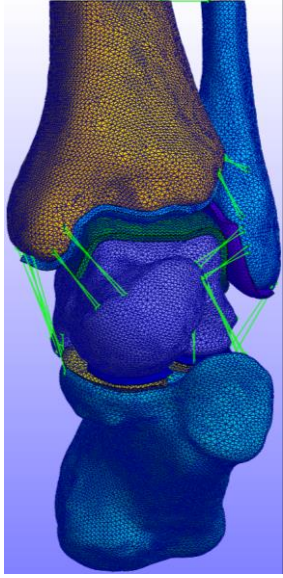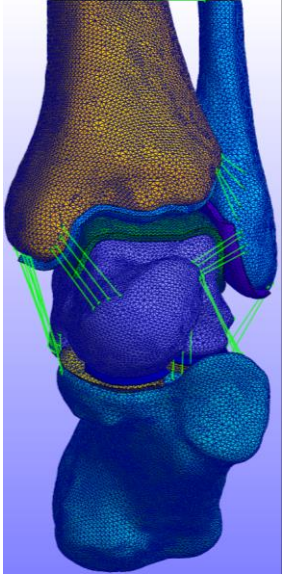
	Model 1	Model 2	Model 3	Model 4
3D-FE MODEL				
	Model 5	Model 6	-	-
3D-FE MODEL			-	-

Figure 10 Ankle complex joint modeled with tibia, fibula, talus, calcaneus, and 12 springs, anterior tibiotalar (ATT), posterior tibiotalar (PTT), anterior talofibular (ATaF), posterior talofibular (PTaF), tibioncalcaneal (TiC), calcaneofibular (CF), anterior tibiofibular, posterior tibiofibular, cervical, talocalcaneal interosseous, lateral talocalcaneal, post talocalcaneal, and medial talocalcaneal. The springs were set in six different ligament morphologies (such as parallel or X-configuration).

CHAPTER III

RESULTS

3.1 Talocrural Joint 1- Two Bone Model (Tibia and Talus)

Six different boundary conditions were applied on a tibia to analyze Talocrural Joint 1 with a sliding contact interface between the tibia and talus. However, the FE model did not converge with the six different represenations of ligament mophorogy and any boundary conditions, as shown Table 7. Thus, tied contact interface has been applied between the tibia and talus instead of a sliding contact interface. The result of stress contour are shown in Figure 11. The maximum stress was measured 0.9624 MPa.
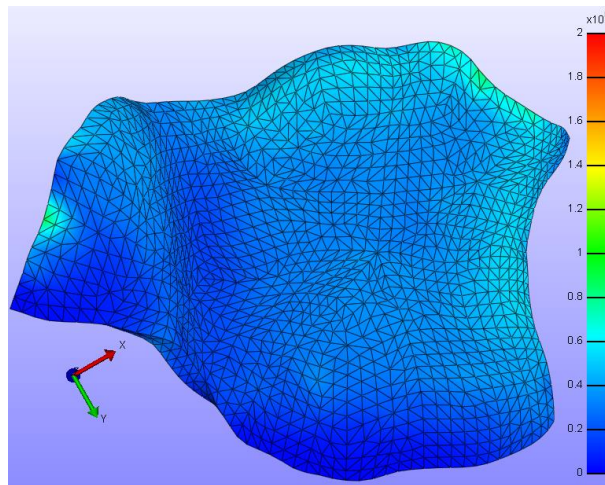
Figure 11 The results of stress contour for two bone FE models using a tied contact interface.

Table 7 The listing for boundary conditions. The talocrural joint was simulated with six different boundary conditions on a tibia to simulate the FE model. Also, the tied contact interface was applied on the tibia as well.

Number of trials	Bone models	Boundary condition	Converged
1st Trial	Tibia	None	No
	Talus	Fixed 6 DoF	
2nd Trial	Tibia	Fixed X	No
	Talus	Fixed 6 DoF	
3rd Trial	Tibia	Fixed XY	No
	Talus	Fixed 6 DoF	
4th Trial	Tibia	Fixed XY and Rz	No
	Talus	Fixed 6 DoF	
5th Trial	Tibia	Fixed XY and RyRz	No
	Talus	Fixed 6 DoF	
6th Trial	Tibia	Fixed XY and RxRyRz	No
	Talus	Fixed 6 DoF	
7th Trial (Tied Interface)	Tibia	None	Yes
	Talus	Fixed 6 DoF	

3.2 Second Model Iteration-Three Bone Model (Tibia, Fibula, and Talus)

The tibia and fibula were fixed in X-direction at the edge of top surface. The talus was also fixed in all six degrees of freedom (DoF) (Table 4). The stress contour as shown in Figure 12 was observed in the cartilage of tibia. The most stress concentration was located in anterior area and the edge of the cartilage at the anterial and lateral areas. Also, the contour plots for contact stress for six different models can be seen in Figure 13. The maximum stresses ranging from 2.3075 MPa to 2.3077 MPa were observed for the three bone model. However, the peak contact stresses were measured 2.3076 MPa in Model 1 through Model 4. The stresses were measured 2.3075 MPa and 2.3077 MPa in Model 5 and Model 6 (Table 8).

Figure 12 Inferior views of a tibia's cartilage. Three bone FE model contact stress for the neutral position with an axial nodal force 600 N. The pick stresses ranging from 2.3075 MPa to 2.3077 MPa were observed in the second model iteration.

Model 1	Model 2	Model 3
Model 4	Model 5	Model 6
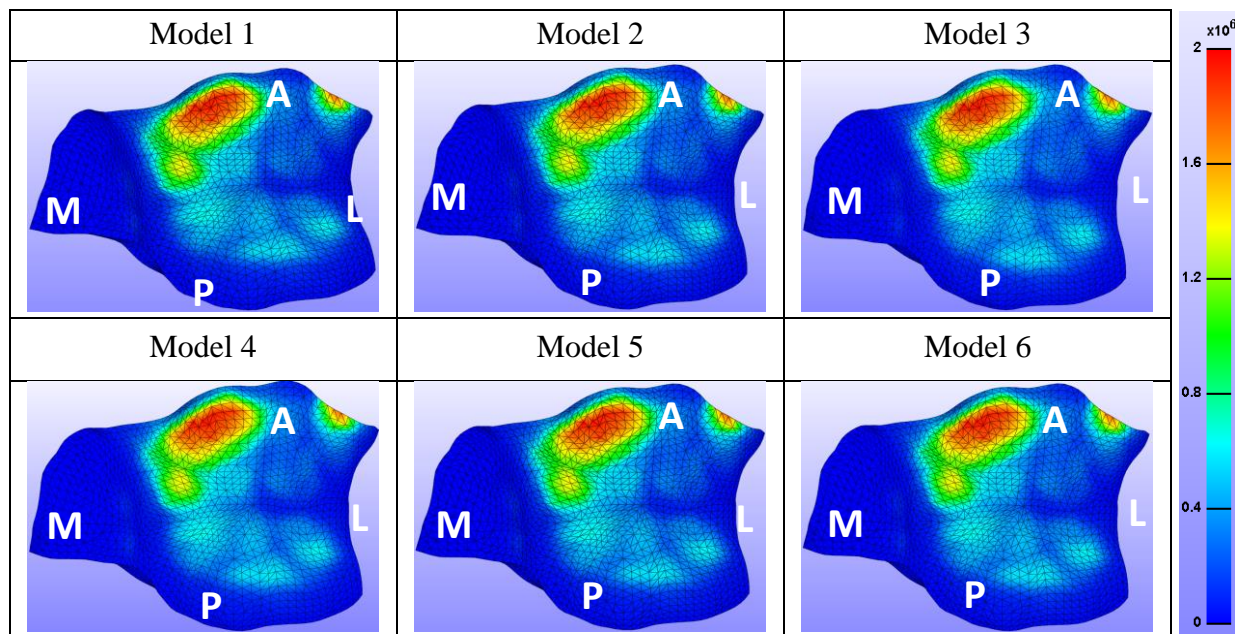
Figure 13 The Inferior views of the tibia's cartilages for six different spring morphologies, respectively. FE contact stress at neutral position with an axial nodal force of 600 N. Legend: A-Anterior; P- Posterior; L – Lateral; M- Medial

Table 8 The maximum and average contact stress in the tibial surface for six different spring morphologies FE model under 600N axial nodal force in the Talocrural Joint 2 model.

	Model 1	Model 2	Model 3	Model 4	Model 5	Model 6
Peak Stress (MPa)	2.3076	2.3076	2.3076	2.3076	2.3075	2.3077
Average Stress (MPa)	1.8822	1.8822	1.8822	1.8822	1.8822	1.8823
Computation Time (minutes)	0:08:36	0:08:08	0:09:13	0:09:08	0:08:34	0:08:38

3.3 Ankle Complex Joint – Four Bone Model (Tibia, Fibula, Talus, and Calcaneus)

The tibia and fibula were fixed in an X-direction at the edge of the top surface. The calcaneus was also fixed in all six DoFs (Table 4). The stress contour, as shown in Figure 14, was observed in the tibia's cartilage. The stress concentration was similarly located in anterior area and the edge of the cartilage at anterior and lateral area. However, the stress concentration in the anterior area was reduced and the stress concentration at posterior area was increased in relationship to the three bone model including the tibia, fibula, and talus. The contour plots for contact stress for six different spring morphologies models can be seen in Figure 15. As a result, the maximum stresses ranging from 2.0541 MPa to 2.0542 MPa were observed in the tibial cartilage surface. However, the peak contact stresses were measured 2.0542 MPa in Model 1 through Model 3 and Model 5. The stresses was measured at 2.0541 MPa in Model 4 and Model 6 (Table 9).
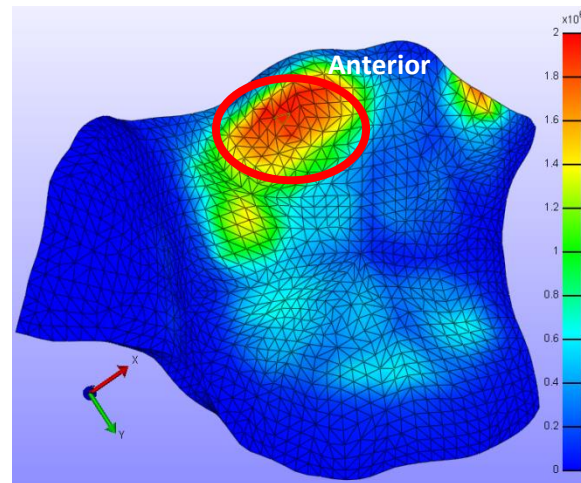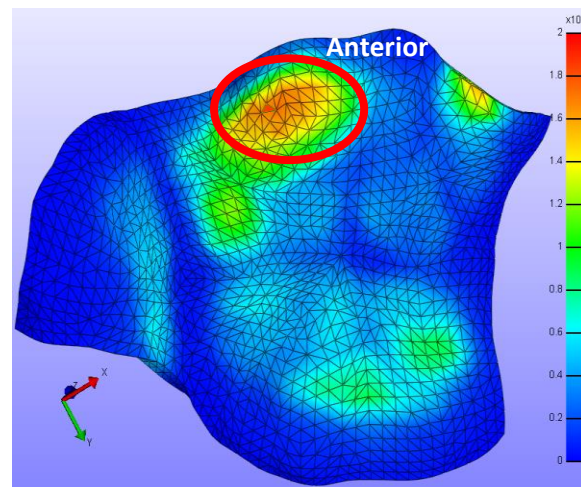

Figure 14 The inferior views of a tibia's cartilage. Ankle complex joint FE model contact stress for the neutral position with an axial nodal force 600 N. The pick stresses was ranging from 2.0541 MPa to 2.0542 MPa were in the ankle complex joint.
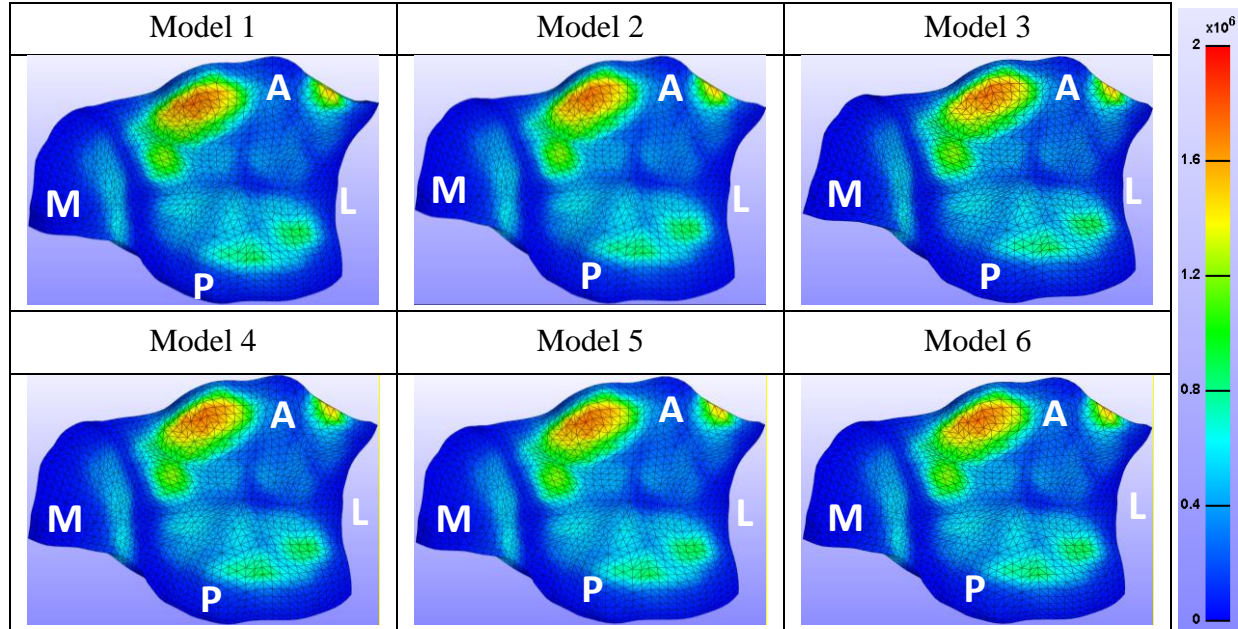
Figure 15 Inferior views of the tibia's cartilages, respectively. FE contact stress for neutral position with an axial nodal force of 600 N. Legend: A – Anterior; P- Posterior; L – Lateral; M – Medial

Table 9 The maximum and average stress in the tibial surface for six different spring morphologies; FE model under 600N axial nodal force in ankle complex joint model.

	Model 1	Model 2	Model 3	Model 4	Model 5	Model 6
Peak Stress (MPa)	2.0542	2.0542	2.0542	2.0541	2.0542	2.0541
Average Stress (MPa)	1.6260	1.6260	1.6260	1.6259	1.6260	1.6259
Computation Time (minutes)	0:13:15	0:12:07	0:11:59	0:12:14	0:12:18	0:11:55

CHAPTER IV

DISCUSSION

Lately, there has been a trend toward developing foot models using computational methods to examine the role of bone structures and tissue such as muscle, tendon, and ligaments. Accordingly, the purpose of this study was to investigate the effect of the number of bones. Similarly to studying the role of ligaments, different morphologies and number of ligaments were applied to three different FE models using a linear elastic spring. Thus, the FE model was developed to improve the understanding of how modeling ligaments and bones affects a simulation. The FE model developed in the open source finite element software developed for biomechanics, FEBio, was evaluated by using three different configurations such as Talocrural Joint 1 based on a tibia and talus, Talocrural Joint 2 based on a tibia, fibula, and talus, and an ankle complex joint which was modeled with a tibia, fibula, talus, and calcaneus. The six different morphologies of ligaments were also applied to each bone configuration.

In 2007, Anderson et al. verified and validated a finite element model including two bones (tibia, talus, and one spring). However, the FE model did not represent physiological conditions [8]. Thus, the current study started with the idea to predict the result of stress, strain, and pressure by changing the bone structures and ligaments as well as to see how boundary conditions are affected by the number and the morphologies of ligaments. The results of the current study were affected by the number of bones and how the ligaments were modeled.

4.1 Bone Segments

The results of the current study indicated that the number of bones in an ankle joint has influence on maximum stress and stress distribution in tibia and talus. Also, the three FE models with sliding contact interface were compared with other person's models. The measured results by Anderson et al., D. Rodrigues, and Liang Dong were shown in Figure 16. As aforementioned in the introduction, the measurement were obtained under different circumstances such as different bone configurations, different number of ligaments, and other tissues. Now the three results were compared with the results of current study in each case.
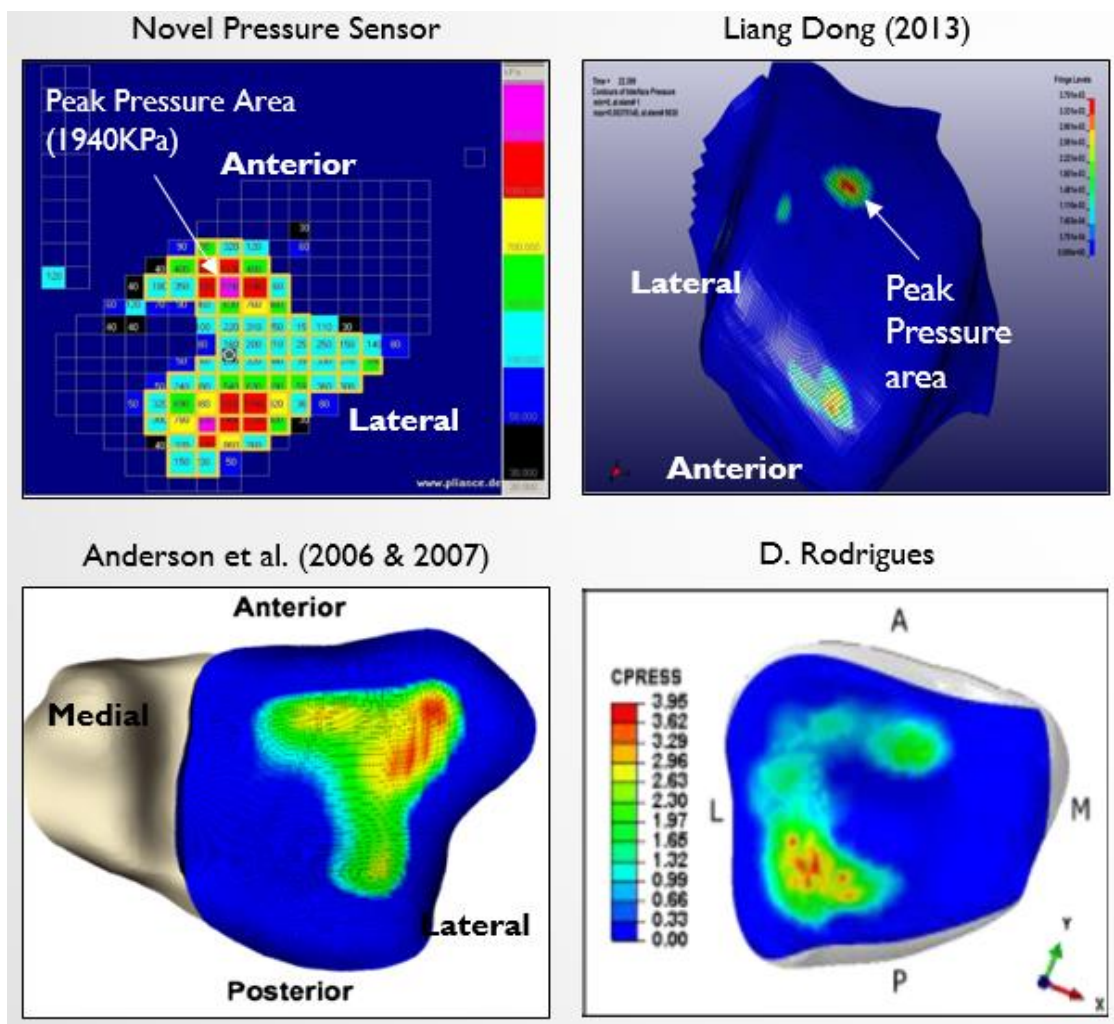
Figure 16 The stress contours ([8, 10, 11]).

Talocrural Joint 1 including tibia, talus, and six different spring morphologies was simulated, but Talocrural Joint 1 did not converge with the sliding contact interface. Thus, the tied contact interface was applied to the three different FE models to investigate the effects on the fibula and calcaneus in the FE models. As a result, the stress contours showed a smaller stress concentration (Figure 16). In both cases, the stress was acting on the edge of cartilage. However, Talocrural Joint 1 had higher stress at the center area than the other FE models. The maximum stresses are 0.9662 MPa and 0.5226 MPa for Talocrural Joint 1 and Talocrural Joint 2 and Talocrural Joint 3.

| Talocrural Joint 1 – Tibia and Talus | Talocrural Joint 2 & 3– Tibia, Talus, Fibula, or calcaneus |
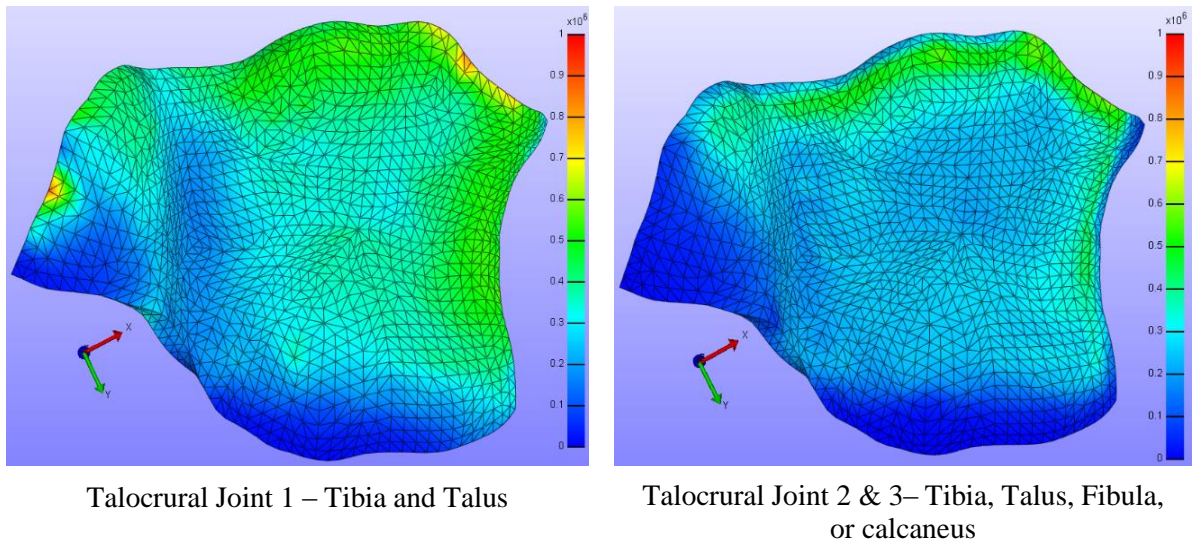
Figure 17 The tied contact interface applied on articular joint to investigate the effects on the fibula.

Table 10 Comparison of the stresses reported in the study.

	Present Study	**Anderson et al. [8]**	**Rodrigues [10]**	**Dong [11]**
Bones	Tibia Talus Fibula Calcaneus	Tibia Talus	Tibia Talus Fibula Calcaneus	Full Ankle
Load	600N Axial nodal load	600N Pressure load	600N Axial nodal load	175N Pressure load
Springs	6 or 12	1	8	6
Results	2.0 MPa ~ 2.3 MPa	2.74 MPa ~ 3.74 MPa	3.95 MPa	2.55 MPa

The stress ranging from 2.0541 MPa to 2.3077 MPa were measured in the Talocrural Joint 2 including the tibia, talus, and fibula, and Talocrural Joint 3 including the tibia, talus, fibula, and calcaneus (Table 10). Anderson et al. and Rodrigues also reported the contact stress 3.69 MPa and 3.95 MPa [8, 10]. Dong reported 2.55MPa contact pressure because Dong applied 175N instead of 600N, and included more bones, and tendon loads [11]. The stress contours were also produced as shown in Figure 16. The stress contours showed some different patterns in each study. In the present study, the most stress was concentrated at anterior and medial side along the edge line of the cartilage in the Talocrural Joint 2 and Talocrural Joint 3 (Figure 18). Specifically, the small amount of stress was moved from anterior to posterior area along median plane when the calcaneus was added to the FE model. When adding the calcaneus to Talocrural Joint 2, the stress was decreased from 2.3 MPa to 2.0 MPa at anterior area. However, the stress was increased from 0.652 MPa to 0.925 MPa. In the results of Anderson et al. using a tibia, talus, and a single spring and Rodrigues using a tibia, talus, fibula, calcaneus, and 8 springs, the stress distribution contours were different. The stress distribution of Anderson et al. was distributed as shown in Figure 16. The mirror symmetrical stress distribution observed in the model by Rodrigues may have occurred because of the different loading conditions, bone configurations, and ligaments. The FE model of Anderson et al. was modeled with a tibia, talus, and one single spring. However, the FE model of the present study was modeled with tibia, talus, fibula, calcaneus, and 6 springs or 13 springs. The 600N pressure load was applied on the tibia in Anderson et al., but a 600 N axial nodal load was applied on the edge of the tibia and fibula. Also, the boundary condition in the Anderson et al. study used fixed plantar and dorsiflexion. Inversion and eversion was free to rotate. However, the talus or calcaneus were fixed at 6

degrees in the present study. This may be one reason why the present study had mirrored symmetrical stress distribution when compared to Anderson et al.

The stress distribution contour in the model developed by Rodrigues has shown that the stress concentration was located at the corner of posterior and lateral area. The maximum stress of Rodrigues was similar with Anderson et al., but the stress contour was different. The difference may have occurred by the number of bones; Anderson's model included 2 bones, Rodrigues' model included 4 bones), boundary condition, loading condition, and ligaments (1 ligament vs. 8 ligaments). Also, a 600N force was applied as an axial nodal force. The reasons for the differences in the models results may be due to the different properties of bone and ligaments and different boundary conditions. Rodrigues used isotropic linear elastic material properties ($E = 19000$ MPa or 500 MPa, $v = 0.3$). Cartilage was modeled as a isotropic linear elastic material properties ($E = 1$ MPa, $v = 0.4$) [10]. However, in the current study, the isotropic linear elastic material ($E = 13000$ MPa, $v = 0.3$) for bones and neo-Hookean ($E = 12$ MPa, $v = 0.42$) was applied. Unfortunately, the boundary condition was not compared because boundary condition was not explained in detail.

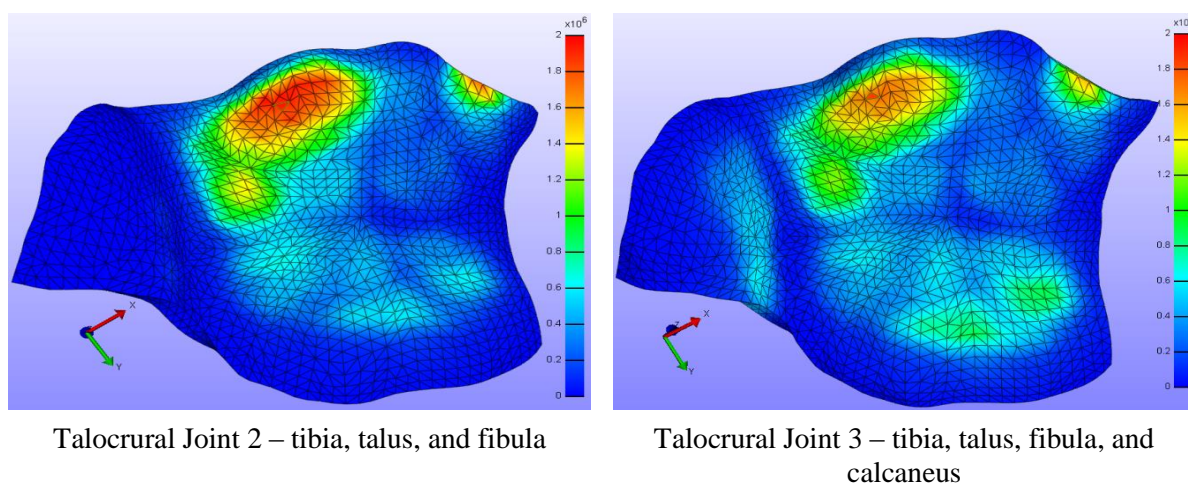Talocrural Joint 2 – tibia, talus, and fibula   Talocrural Joint 3 – tibia, talus, fibula, and calcaneus

Figure 18 Results of stress contours for Talocrural Joint 2 and Talocrural Joint 3.

4.2 Ligaments (Spring)

In anatomy, the ankle consists of several ligaments, but the properties of ligaments did not have enough data to apply the stiffness of ligaments. During this study, the stiffness of ligaments found in the literature was 10-100 N/mm. For the ligaments that were missing data, the stiffness was 40 N/mm because the selected stiffness was the minimum stiffness in which the FE model converged. Also, the position of ligaments was not defined, so the positios of ligaments was chosen based on knowledge of anatomy, and a sensitivity analysis of the position was not conducted. As the number of springs increased, the results of stress and stress contour were not changed, but the computational time decreased. The computational time was 13 minutes 15 seconds with a single spring in each ligament. However, adding more springs and changed the morphology of each ligament and the computational time ranged from 11 minutes 55 seconds to 12 minutes 18 seconds.

4.3 Limitations

In this study, the CT scan images were used to investigate FE model of a foot. However, the CT images were collected by others and the images were segmented manually, so some physical error could have occurred. The material properties of ligaments were obtained from the literature based on data from a small number of cadavers, and some of the ligament material properties were not measured. Therefore, the ligament properties may have caused errors in the results. Similarly, the cartilage properties were obtained from the literature and could contribute to errors in the model. The locations for each ligament were selected based on knowledge of anatomy because they were not able to be identified on the CT images. Furthermore, the cartilage in an ankle joint has a mean thickness in the range of 1 to 2.38 mm, but in this study, the cartilage was assumed to be a uniformly thin layer about 1.77mm. Additional limitations were axial load and

different ankle angles. In this study, off-axial load was not modeled and the different ankle angles such as dorsiflexion, plantar flexion, eversion, and inversion were not investigated.

4.4 Future Work

In this study, a FE model which consisted of a tibia, talus, fibula, and calcaneus was only simulated in the neutral position. The dorsiflexed and plantarflexed positions were not analyzed. For the next study, the two positions should be analyzed to study stress distribution during gait movement. The stiffness and location of ligaments were unknown because of a lack of reference, so the properties of ligaments should be proved scientifically.

Furthermore, in this study, tendon, skin, and others were not included. To understand changing stress of anatomical ankle, the FE model should include the tendon, skin, and others. The last one to improve the FE model, the CT scan data should be considered to minimize the errors. Then, additional work would be necessary for the stress analysis on ligaments in which stress is mostly exerted on the posterior tibiotalar and the intersosseous talocalcaneal.

CHAPTER 5

CONCLUSIONS

The aim of this study was to determine how modeling the morphology of the ligaments and the number of bone affects stress or pressure. AFE model of the ankle was initially developed to analyze and predict cartilage stresses between the tibia and talus during the stand phase of gait with ligaments. Three different 3D FE models with six different spring morphologies in each FE model were developed for the comparison of stress and stress contours. In this study, the effect of the number of bones and ligaments has been mainly investigated. It proves that the stress between tibia and talus was dependent on the number of bones. The six different morphologies of ligaments with axial load did not affect the result of stress and stress contour in each FE model, but the computational time decreased. Additionally, for limitations and future work, the current FE models were constructed with13 ligaments chosen based on knowledge of anatomy. Thus, the locations of ligaments should be considered when CT data are compiled to create a finite element model. Also, the off-axial load and the different ankle angles (i.e., dorsiflexion, plantar flexion, inversion, and eversion) should be considered to classify the effect of the number of bone and morphology of ligaments during gait.

REFERENCES

[1]   K. D. Button, F. Wei, E. G. Meyer, and R. C. Haunt, "Specimen-specific computational models of ankle sprains produced in a laboratory setting," *Biomechanical Engineering,* vol. 135, p. 6, 2013.

[2]   M. Aurich, G. O. Hofmann, B. Rolauffs, and F. Gras, "Differences in injury pattern and prevalence of cartilage lesions in knee and ankle joints: A retrospective cohort study," vol. 6:5611, p. 4, 24 August 2014.

[3]   Z. Jin, "Fundamentals of computational modelling of biomechanics in the musculoskeletal system," p. 9, 2014.

[4]   S. Jacob, K. M. Patil, L. H. Braak, and A. Huson, "Stresses in a 3D two arch model of a normal human foot," vol. 23, p. 7, 1996.

[5]   J. SHIN and N. YUE, "A finite element model of the foot and ankle for automotive impact applications," *BMES,* vol. 40, p. 13, December 12 2012.

[6]   A. L. Boskey and R. Coleman, "Aging and bone," p. 16, 2010.

[7]   R. M. Koch, M. H. Gross, and F. R. Carls, "Simulating facial surgery using finite element models," p. 8.

[8]   D. D. Anderson, J. K. Goldsworthy, W. Li, M. J. Rudert, Y. Tochigi, and T. D. Brown, "Physical validation of a patient-specific contact finite element model of the ankle," *Journal of Biomechanics,* vol. 40, pp. 1662-1669, January 27 2006.

[9]   Wikipedia.org (July 11, 2017). *Anatomical terms of motion*. Available: https://en.wikipedia.org/wiki/Anatomical_terms_of_motion#/media/File:Dorsiplantar.jpg

[10]   D. Rodrigues, "Biomechanics of the total ankle arthroplasty: Stress analysis and bone remodeling," p. 10.

[11]   L. Dong, "Prelimnary development of a subject specific finite element model of the hindfoot," Master of Science, Mechanical Engineering, Old Dominion University, 2013.

[12]   S. A. Millington, M. Grabner, R. W. Mag, and D. D. Anderson, "Quantification of ankle articular cartilage topography and thickness using a high resolution stereophotography system," *Osteoarthritis Research Society International,* vol. 15, p. 7, 2007.

[13]   L. S. T. CORPORATION. LS-DYNA® KEYWORD USER'S MANUAL [Online].

[14]   R. Alberson, D. Sgtevens, J. D. Walker, and T. Moore, "AutoMesher for LS-DYNA Vehicle Modeling," presented at the 13th International LS-DYNA Users Conference, Dearborn, MI, 2014.

[15]   F. Wei, J. E. Braman, B. T. Weaver, and R. C. Haut, "Determination of dynamic ankle ligament strains from a computational model driven by motion analysis based kinematic data," *Journal of Biomechanics,* vol. 44, p. 6, 16 August 2011.

[16]   S. Maas, D. Rawlins, D. J. Weiss, and D. G. Ateshian, "Finite elements for biomechanics (FEBio)-Manual," Version 2.5 ed. Salt Lake City, Utah, 2016.

[17]   S. A. Maas, B. J. Ellis, G. A. Ateshian, and J. A. Weiss, "FEBio: Finite elements for biomechanics," *Biomechanical Engineering,* vol. 134, p. 10, 2012.

[18]   K. D. Butz, D. D. Chan, E. A. Nauman, and C. P. Neu, "Stress distributions and material properties determined in articular cartilage from MRI-based finite strains," *Journal of Biomechanics,* vol. 44, p. 6, 2011.

[19]   T. M. Hoagland and T. R. Gest. Ankle joint anatomy [Online]. Available: http://emedicine.medscape.com/article/1946201-overview

[20]   W. R. Ledoux, C. Mkandawire, B. J. Sangeorzan, and R. P. Ching, "Foot and ankle ligament morphometry," *JRRD,* vol. 42, p. 11, November/December 2005.

[21]   R. Wenny, D. Duscher, E. Meytap, P. Weninger, and L. Hirtler, "Dimensions and attachments of the ankle ligaments: Evaluation for ligament reconstruction," vol. 90, p. 11, 2014.

[22]   S. Siegler and J. Block, "The mechanical characteristics of the collateral ligaments of the human ankle joint.," JOURNALNAME??? p. 9, 1988.

[23]   C. W. Imhauser, "The development and evaluation of a 3-dimensional, image-based, patient-specific, dynamic model of the hindfoot," Doctor of Philosophy, Drexel University, 2004.

VITA

Jinhyuk Kim

EDUCATION

Master of Science in Mechanical Engineering at Old Dominion University, August 2014-August 2017. Thesis title: "The effect of bone and ligament morphology of ankle joint loading in the neutral position."

Bachelor of Science in Mechanical Engineering, Old Dominion University, Norfolk, Virginia

ACADEMIC EMPOYMENT

Graduate Teaching Assistant, Department of Aerospace and Mechanical Engineering, Old Dominion University, August 2014 – present. Responsibilities include: assisting professors with the preparation and presentation of undergraduate courses, grading, and tutoring.

ACADEMIC AWARDS

2014 Student Employee 1st Runner up From Old Dominion University (2014)

Veterans of the Korean War Reunion Educational Assistance Award (2013)